ECCOMAS Congress 2016
VII European Congress on Computational Methods in Applied Sciences and Engineering
M. Papadrakakis, V. Papadopoulos, G. Stefanou, V. Plevris (eds.)
Crete Island, Greece, 5–10 June 2016

SEISMIC ASSESSMENT OF A 5-STOREY RETROFITTED RC BUILDING

Hussein Bark[1], George Markou[1], Christos Mourlas[2] and Manolis Papadrakakis[2]

[1] ALHOSN University, Department of Civil Engineering
P.O.Box 38772, Abu Dhabi, UAE
habark01@students.alhosnu.ae, g.markou@alhosnu.ae

[2] Institute of Structural Analysis & Seismic Research, National Technical University of Athens
9 Iroon Polytechniou Str.,Zografou Campus,GR-15780 Athens,Greece
mourlasch@central.ntua.gr, mpapadra@central.ntua.gr

Keywords: Retrofitted Structure, Reinforced Concrete Modeling, Finite Element Method, Seismic Assessment.

Abstract. *Due to severe damages on structures caused by earthquakes different approaches were introduced to enhance their carrying capacity. The most common one is retrofitting, which is a technique used to improve the structural capacity of a building that is found to be inadequate against earthquake loads. The problems that arise when retrofitting reinforced concrete structures, is the use of objective and sound methods that will provide the engineer with the tools to assess the final design. This work aims to alleviate this restriction by performing a complete study of a 5-storey reinforced concrete structure that was retrofitted with reinforced concrete shear walls through the use of 3D solid finite elements. Cracking is treated with the smeared crack approach and the steel reinforcement is simulated by embedded rod elements. This detailed modeling approach is applied for the first time so as to perform a full pushover analysis of a 5-storey RC retrofitted building. The numerical results illustrate that the proposed assessment approach is computationally accurate. Furthermore, the use of parallel processing is required so as to decrease the computational demand when dealing with full scale models.*

1 INTRODUCTION

Retrofitting is required under several circumstances according to [1], especially when not taking into account the additional seismic loads while designing. Retrofitting is applied on existing structures that were designed according to old seismic codes, thus their lateral strength is not sufficient to carry the expected seismic forces. Moreover, building with poor construction quality can be enhanced as well.

There are mainly two types of retrofitting, global and local. The global retrofitting is concerned with the seismic resistance of a structure by placing shear walls, infill walls, steel bracings, and base isolation [2]. On the other hand, the techniques that increase the carrying capacity of inadequate members locally are considered as local strengthening methods. This includes reinforced concrete (RC), steel or fiber reinforced polymer (FRP) jacketing of the existing members such as columns, beams, joints, walls and foundations [3]. Selecting the appropriate retrofitting strategy is based on economy, performance and constructability. Sometimes it is more preferable to use more than one technique in a single structure

When it comes to design the retrofitted structural member, the available methods are rather limited given that semi-empirical formulas available in design codes account for the behavior of the section but do not integrade the effect on the overall mechanical behavior of the structure and its derived capacity after the retrofitting has been implemented locally. As it will be shown in this research work, the prementioned restrictions can be alleviated through the use of state-of-the-art 3D detailed finite element modeling.

2 NUMERICAL METHOD USED

The numerical method that was used in this research work was the Finite Element Method (FEM) [4]. In order to determine the mechanical behavior of the under study structure, two software have been used: Femap and ReConAn. Below follows a short description of the two finite element analysis software.

2.1 Femap

Femap is an advanced engineering simulation program owned by Siemens PLM Software. It is used as a “pre-processing” tool to construct finite element models and as a “post-processing” tool to display results.

2.2 ReConAn FEA

ReConAn is a research finite element analysis software created at the NTUA [5]. It uses two post-processing programs, Femap and ReConAn Eye. ReConAn Eye is encapsulated inside ReConAn main code structure to illustrate the crack openings that derive from the analysis as smeared cracks.

3 5-STOREY RC BUILDING

The under study building used in this research work was a seismically strengthened 5-storey RC building adopted from Orakdogen et al. [6], where the building was analyzed and studied for the effect of soil structure interaction (SSI) for different foundation types (see also [7]). This RC building is used herein so as to develop the numerical models that will be presented in the next sections.

3.1 Geometry

As it can be seen in Figure 1, the initial framing system of the building consisted of 12 columns (with rectangular sections of 25x40cm) and drop-beams (15x50cm) supporting the slabs (10cm of thickness). The initial framing system was strengthened by constructing four main shear walls (two shear walls parallel to the x axis and two parallel to the y axis) around the existing columns (Figure 1). The total length and width of the building's plan are 10.2m and 6.8m, respectively, while the total building height is 13.9m (the ground floor height is 2.15m, 3 typical floors have a 2.75m height each and the top floor has a height of 2.5m) [6].

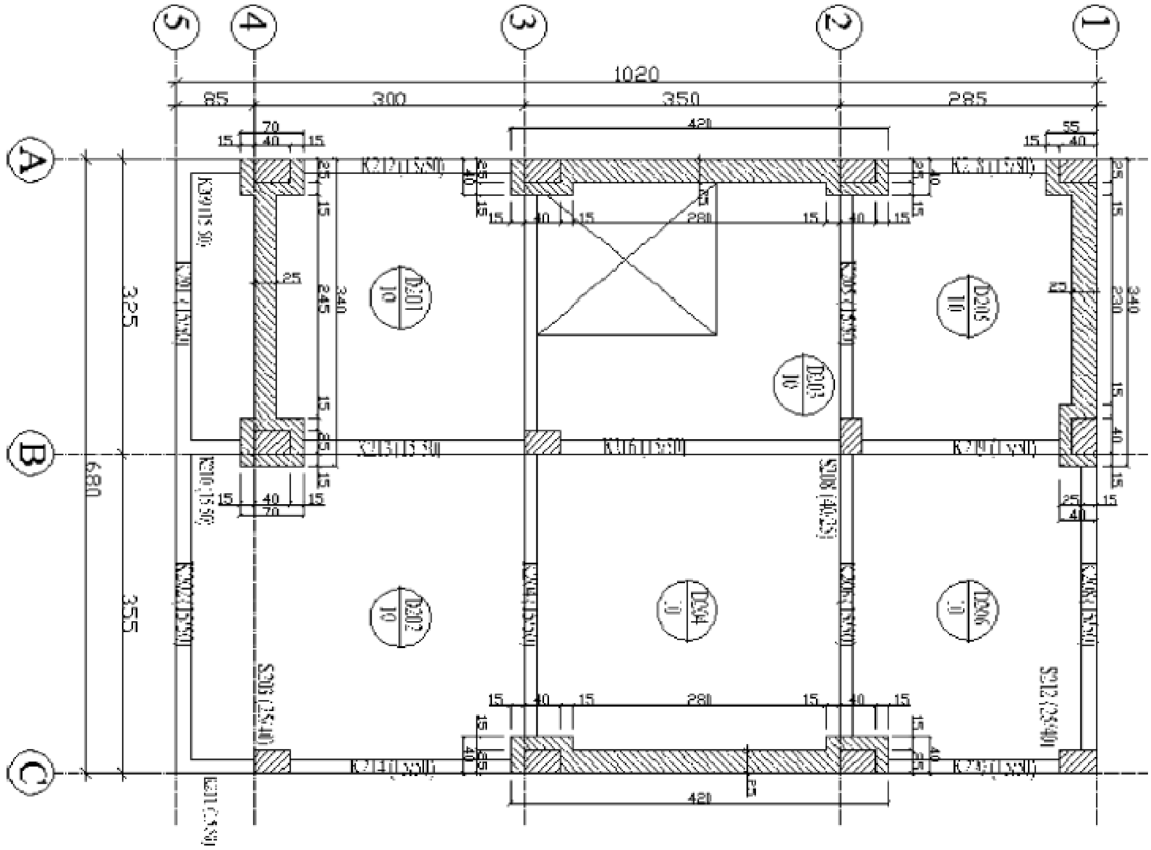

Figure 1: RC 5-storey building typical plan view [6]

3.2 Material properties

The material properties of the structure are divided into: (a) existing RC material, where the uniaxial compressive strength of concrete was reported to be equal to 16MPa and the steel reinforcement that had a yielding stress of 220 MPa, (b) the RC material used to strengthen the building (infill walls) had 20MPa and 420MPa, uniaxial concrete compressive strength and steel yielding stress, respectively. These were also the values incorporated in the numerical models presented below.

4 NUMERICAL MODELS

Two models were developed so as to study the overall effect of retrofitting. Model A foresees the discretization of the initial frame and Model B the discretization of the retrofitted frame. 20-nodded hexahedral elements where used in order to discretize the concrete meshes while rod finite elements were used for the embedded rebars. Different colors where used so as to distinguish between different rebar diameters. Also steel plates (2cm thick) were used for the application of the external horizontal load in order to avoid any local failure. It must be noted here that the slabs were modeled through the use of a von Mises material model in an attempt to decrease the computational demand of the models. The concrete uses a 3D constitutive matrix as presented by Kotsovos and Pavlovic [8] and later modified by Markou and Papadrakakis [9].

4.1 Initial model (Model A)

Table 1 shows the reinforcement details for each structural member of the building.

Element	Properties
Beams	Rebar: 4Ø12 Stirrups: Ø8/15cm
Columns	Rebar: 6Ø14 Stirrups: Ø12/15cm
Footings	Top & Bottom X direction: Ø12/15cm Top & Bottom Y direction: Ø12/15cm

Table 1: Reinforcement details of the initial mode

As stated above, Femap was used in order to create both numerical models (initial and retrofitted frame). The procedure followed for the model construction is summarized in four steps: (a) constructing the concrete mesh, (b) create the embedded rebars inside the concrete mesh, (c) apply the constrains, and (d) apply the loads. The initial model is shown in Figure 2a, where the concrete mesh, the applied loads and the fix support can be seen. Figure 2b shows the embedded rebars mesh, while a zoom view that illustrates the embedded rebars within a RC joint is also shown.

Three types of loads were applied in both models. (a) Dead load: the self-weight of the building which applied automatically by the software, (b) Live load: 3kN/m^2 distributed load were assigned on each slab. (c) Earthquake load: horizontal load was applied along the Y-direction at each floor as shown in Table 2. The pushover analysis foresaw 10 load increments and a convergence tolerance of 10^{-4}.

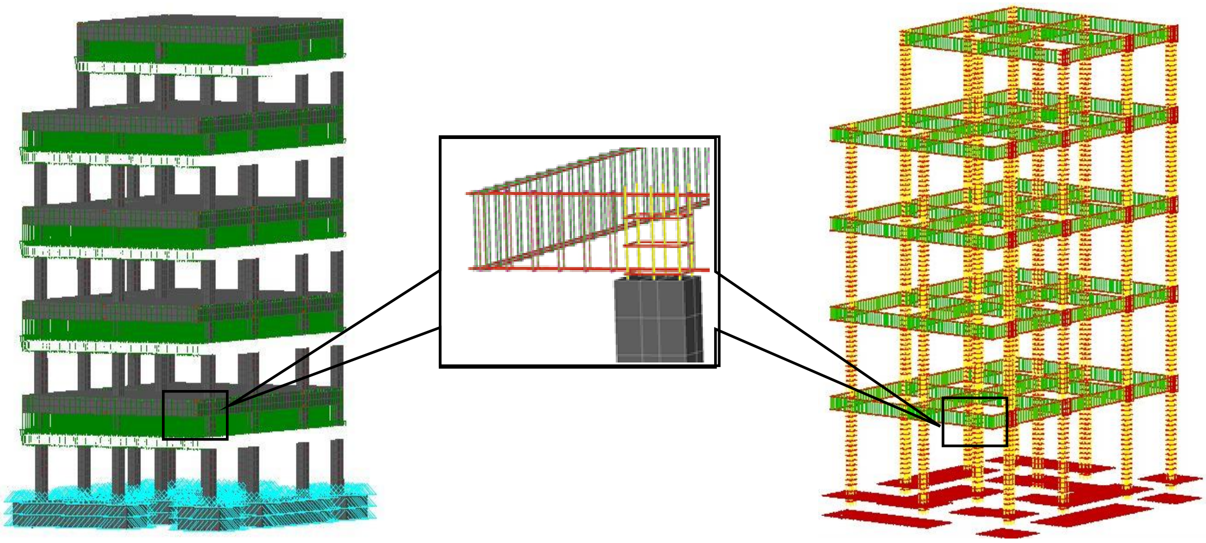

a) b)

Figure 2: Model A. a) Hexa mesh. b) Embedded rebars mesh

Storey number	Earthquake loads (kN)
First	66.67
Second	133.33
Third	200
Forth	266.67
Roof	333.33
Total	1000

Table 2: Earthquake loads distribution

4.2 Retrofitted model (Model B)

As previously mentioned, RC shear walls were used in both directions to improve the overall stiffness and strength of the structure (see Figure 1). The shear walls and RC jackets were reinforced as shown in Table 3. New finite elements were added to Model A without any modifications performed on the initial mesh. Figure 3 and Figure 4 present the mesh of the second model (Model B).

Element	Properties
RC Jackets	Dimensions: 15 cm around columns Rebar: Ø14 at each 15 cm Stirrups: Ø8/15 cm
Shear Wall	Web Rebar: 16ø12 Confinement Rebar: 6Ø20 Stirrups: Ø8/15 cm

Table 3: Rebars used for retrofitting

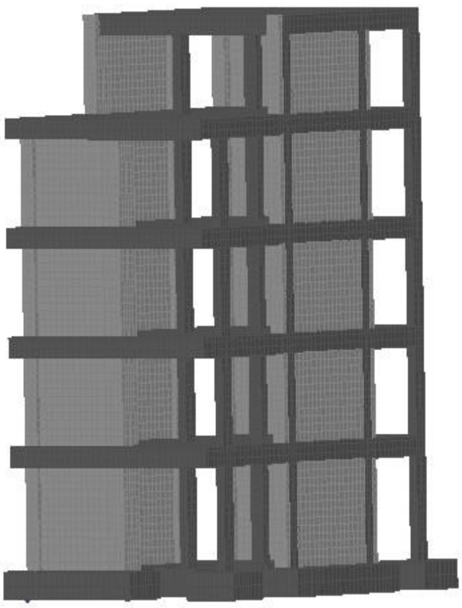

a)

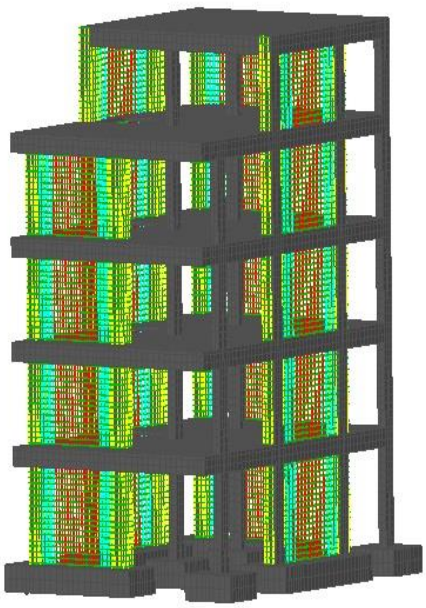

b)

Figure 3: Model B. a) Concrete mesh of the retrofitted structure. b) rebar mesh embedded in the shear walls

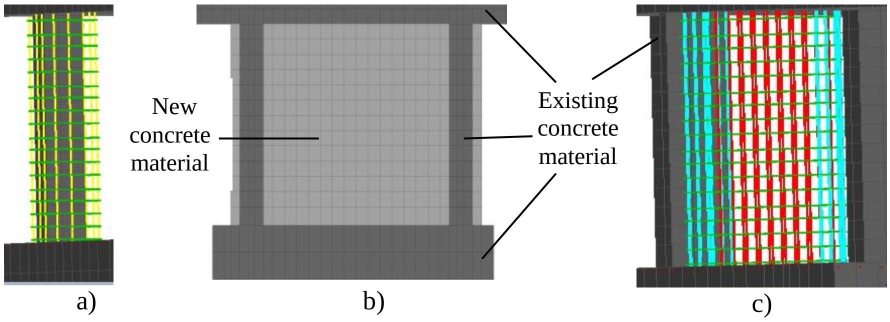

Figure 4: Model B. a) Retrofitting rebars around the column. b) Shear wall concrete mesh with initial columns. c) Shear wall reinforcement mesh

5 NUMERICAL RESULTS AND DISCUSSION

5.1 Analysis of Model A

After constructing the two models, the input data files were exported for analysis through the use of ReConAn FEA. The solution of the entire full-scale model required 29 days, which highlights the excessive computational demand of the problem. So as to assemble and store the stiffness matrix of Model A (Skyline storage), 30Gb of RAM were required. This numerical finding underlines the need of using parallel processing (a research work that is under process), while demonstrates the numerical robustness of the developed algorithm in handling this large-scale numerical problem.

Figure 5 shows the predicted P-δ curve. As it resulted from the numerical analysis, the structure managed to carry a total of 540kN prior complete failure. The failure was attributed to the failure of longitudinal reinforcement at the ground floor columns which initiated an excessive internal forces redistribution leading the frame to failure. The computed capacity does not satisfy the codes demand which was 693-954kN [6] according to the soil conditions.

As it can be seen in Figure 6a, the predicted crack initiation at load increment 1 foresees that the main crack openings are located at the joints of the structure. As the horizontal load increased, the cracks increased in size and number until complete failure (see Figure 6b).

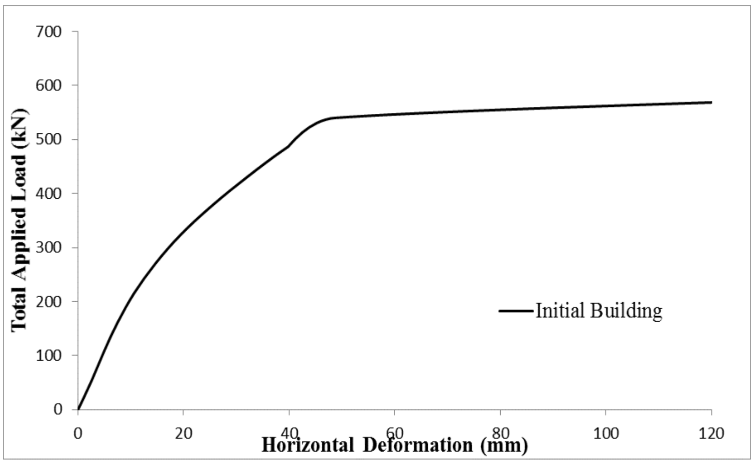

Figure 5: P-δ curve of initial building

5.2 Analysis of Model B

On the other hand, the solution of Model B required 66 days. So as to assemble and store the stiffness matrix of Model B, 37Gb of RAM were required due to the additional FE elements used in order to discretize the retrofitting infill walls. The analysis details are summarized in Table 4 for both models.

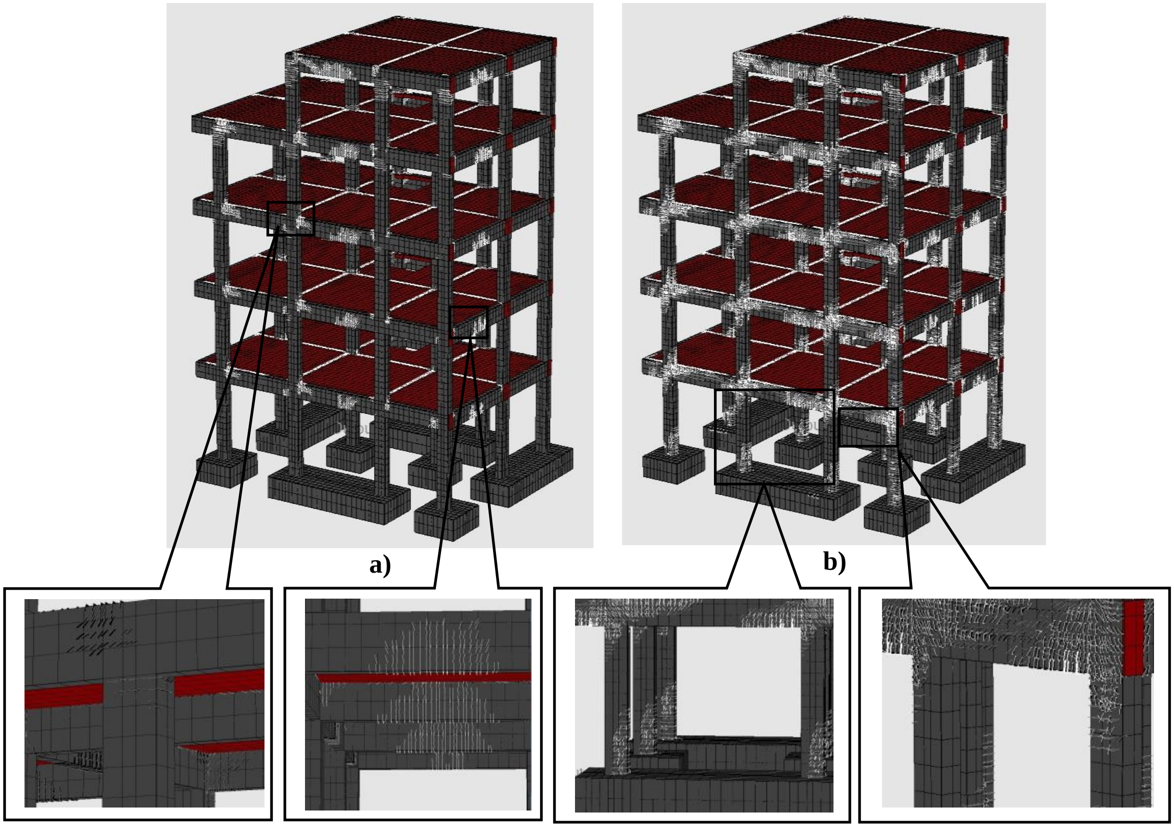

Figure 6: Model A. a) Initial cracks at load increment 1. b) Cracks prior to failure

	Model A	**Model B**
Mesh Data		
Total no. nodes	159,567	240,060
No. hexa elements	19,044	29,431
No. embedded rebars	27,399	58,072
Total no. elements	46,443	87,503
Analysis Data		
No. of stiffness matrix elem.	3,761,459,688	4,688,727,648
Required RAM for the stiffness matrix	30Gb	37Gb
Required RAM for the analysis	36Gb	43Gb
Embedded mesh generation time	10min 14sec	34 min 6 sec
Time for solving nonlinear analysis	29-days	66-days
No. of load incr. solved successfully	6 load incr.	9 load incr.
Time for writing the output data	25min 48sec	1hr 28min
Total computational time	29-days	66-days

Table 4: General numerical details that derived after the nonlinear analysis of the FE models.

As it can be seen in Figure 7a, the results from the pushover analysis of Model B, predicted the initiation of cracks occurred at the beams' end joints due to the moments that were generated from the applied horizontal load. As the horizontal load increases, the cracks increase in size and number until complete failure (see Figure 7b). The shear walls develop horizontal and diagonal cracks as the horizontal load increases (see Figure 7b). The retrofitted model failed due to the rapture of the longitudinal reinforcement of the beams that were connected to the shear wall leading the solution to stop.

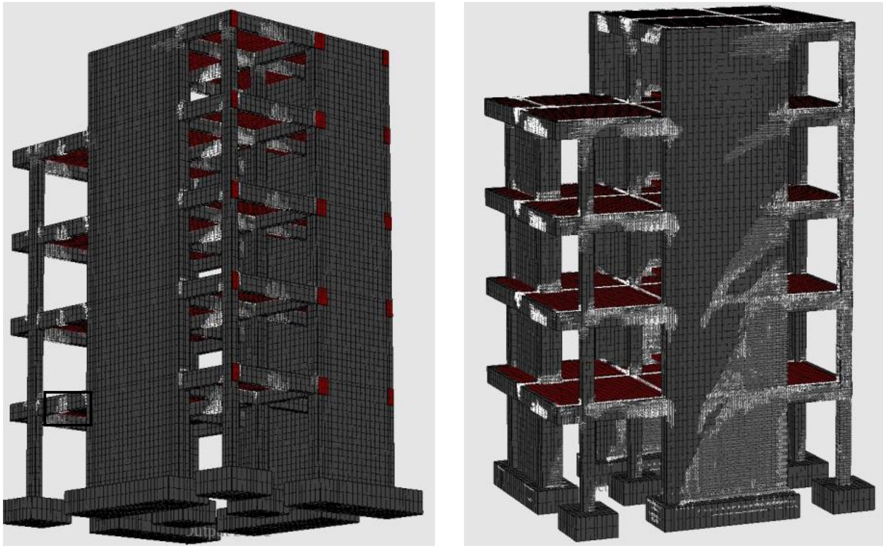

a) **b)**

Figure 7 Model B. a) Initial cracks at load increment 1. b) Cracks prior to failure

Figure 8 shows the comparison between the predicted P-δ curves for both models. As it resulted from the numerical analysis, the strengthened structure managed to carry a total of 1800kN prior complete failure. As mentioned above, the failure was attributed to concentration of strains at the beam-shear wall joints which led the frame to failure. It is also shown that with the increase in the stiffness due to the retrofitting shear walls, the resulted horizontal displacement decreased significantly.

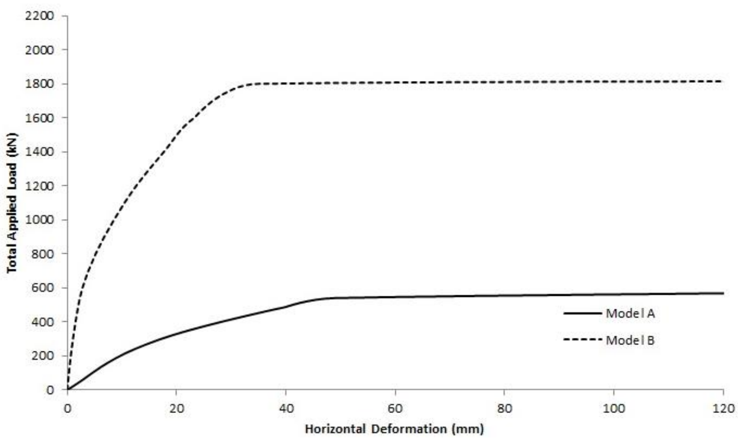

Figure 8: Comparison of P-δ curves for both models (A & B)

	Model A	**Model B**
No. of load increments until failure	6	9
Numerically predicted Base Shear (kN)	540	1800
Max Horizontal Deformation (cm)	5.02	3.94

Table 5: General outputs that derived from the FEA of both models.

Table 5 illustrates the comparison between the numerical results for both models. While Figure 9 shows the von Mises strain contours for both framing systems prior to failure.

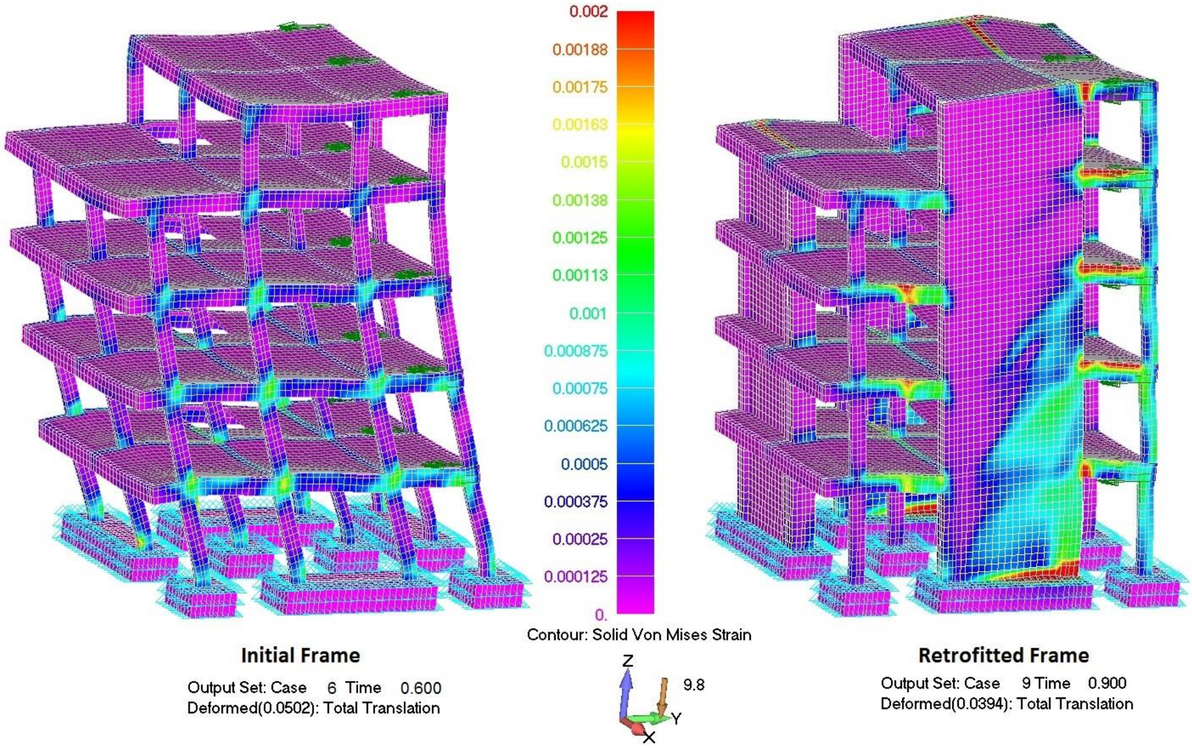

Figure 9: Comparison of von Mises contours for both models prior to failure

5.3 Analysis Results of a Single RC Infill Shear Wall

In order to investigate the overall capacity of the derived shear wall (13.9m height) after the retrofitting, a shear wall model was developed and analyzed until complete failure (see Figure 10). The retrofitting rebars that were used to construct the shear wall were assumed well anchored within the existing framing system, so as to avoid any local failure and capacitate the full strength of the shear wall. Eurocode 2 [10] was used so as to compare the numerically obtained failure load. According to Equations (1) and (2) of EC2, the resulted resistance of the shear wall section was 687kN in shear, and 5880kNm in bending moment. It must be noted here that only the characteristic values were used so as to compute the strength in shear and moment.

$$M_{Rd}= b_w \cdot l_c \cdot \rho_{vc} \cdot f_s \cdot d_1 + b_w \cdot x_u \cdot \rho_{vc} \cdot f_s \cdot d_2 + b_w \cdot (l_c + c - x_u) \cdot \rho_{vc} \cdot f_s \cdot d_3 + b_w \cdot (l_w - 2h_c) \cdot \rho_{vw} \cdot f_s \cdot d_4 + b_w \cdot x_u \cdot 0.8 f_c \cdot d_2 \quad (1)$$

$$V_{Rd,c}=[C_{Rd,c} \cdot k(100 \cdot \rho_l \cdot f_{ck})^{1/3}+k_1 \sigma_{cp}] b_w d \quad (2)$$

Figure 10a represent the crack pattern of the shear wall (Model l) at load increment 1 where a 5% of the horizontal load (30kN) was applied. No cracks were formed until load increment 3 where the model entered the inelastic zone (the total horizontal load was applied incrementally through 20 load increments). The shear wall failed at load increment 19 (95% of the applied horizontal load) as shown in Figure 10. The P-δ curve in Figure 10c shows the overall response of the retrofitted part of the structure as it was obtained from the analysis where it can be seen that the predicted failure load was 540kN, smaller than the load predicted by EC2. This is attributed to the code’s inability to account for the eccentricities that derive additional stresses and strains during the loading procedure, leading the shear wall to a premature failure. When the vertical static loads are applied, the shear wall develops an out of plane initial deformation thus the horizontal loads force the wall to deform in a bending and torsional manner (due to the eccentricity).

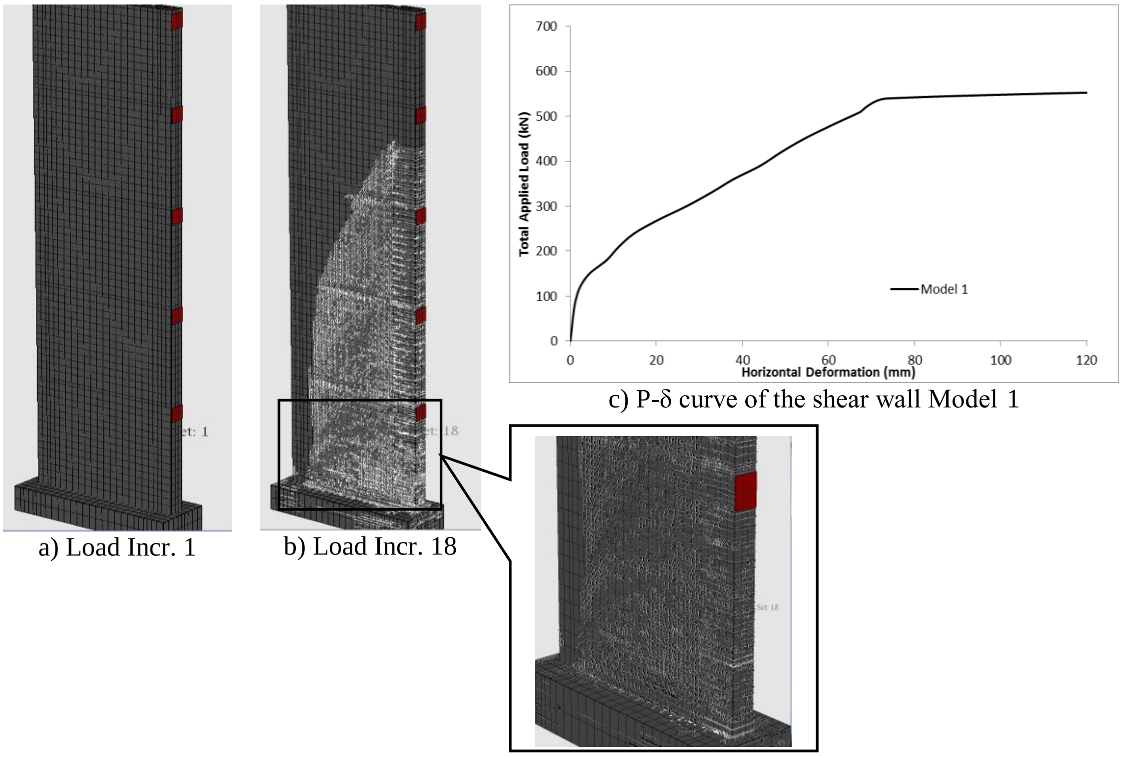

a) Load Incr. 1 b) Load Incr. 18 c) P-δ curve of the shear wall Model 1

Figure 10: Shear wall Model 1 crack patterns and P-δ curve

So as to further investigate the resulted carrying capacity of the shear wall, 5-additional models were developed that foresaw different material properties. The effect of the proper anchorage of the retrofitting rebars was also investigated through this study. Table 6 presents the details of each model that was developed, while Figure 8 illustrates the well anchored reinforcement (Figure 11a) and not anchored reinforcement (Figure 11b).

Model	**Retrofitting concrete (MPa)**	**Retrofitting Steel (MPa)**	**Embedded rebars anchored properly (Yes or No)**	**Numerically predicted Base Shear (kN)**
1	20	420	Yes	540
2	20	420	No	240
3	30	500	No	240
4	30	420	Yes	640
5	20	500	Yes	560
6	30	500	Yes	660

Table 6: Mesh and material details of the shear wall models

Figure 12 shows the crack patterns of the shear wall models prior to failure, where Figure 12b represents the crack pattern that was obtained from Model 1 (see also Figure 10), while Figure 12a and Figure 12c illustrate the crack patterns at load increment 8 (240kN failure load) of Models 2 and 3, respectively. As it resulted from the parametric investigation Models 2 and 3, exhibit a significantly decreased overall strength (see Table 6) due to the fact that the longitudinal reinforcements were not anchored properly (throughout the height of the shear wall). Even in the case of Model 3 where the material properties were increased for both concrete and steel, the shear wall failed prematurely due to local strain concentration (see Figure 12c) that led to significant horizontal cracking (at the area where the longitudinal retrofitting reinforcement were not anchored properly).

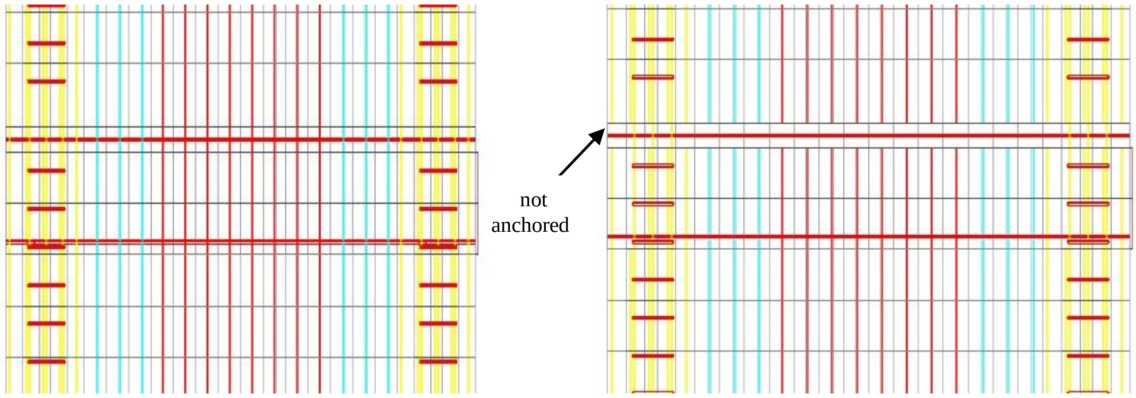

a) Fully anchored longitudinal retrofitting rebars   b) Not anchored longitudinal retrofitting rebars

Figure 11 Anchoring of retrofitted rebars

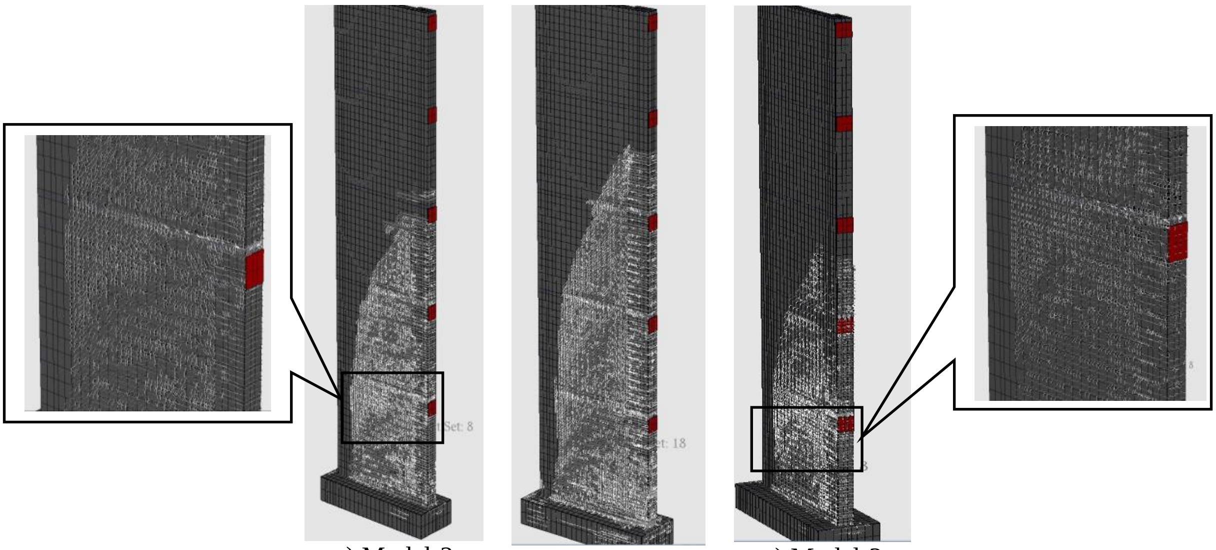

a) Model 2   b) Model 1   c) Model 3

Figure 12: Crack patterns of shear wall models prior to failure (Models 1,2 &3)

Moreover, model 4 that foresaw full anchorage, failed at load increment 16 (640kN), where the crack pattern is shown in Figure 13a. Model 5 (see Figure 13b) managed to carry 560kN, which was attributed to the increased steel yielding strength assumed in comparison to Model 1 (540kN). Figure 13c shows Model 6 that failed for a load of 660kN. This last model resulted the highest capacity given that it foresaw both increased retrofitting material properties and full anchorage of the retrofitting rebars. Figure 14 present the comparison of all numerically obtained P-δ curves.

In order to further investigate the performance of the retrofitted structural member (shear wall), a cyclic analysis was performed by using the shear wall model (Model 1). A history displacement was assigned at the top of the shear wall that foresaw the application of 5 complete cycles (see Figure 15). A displacement of 75 mm was assigned at the top section of the shear wall which was then multiplied by the displacement factor shown in Figure 15.

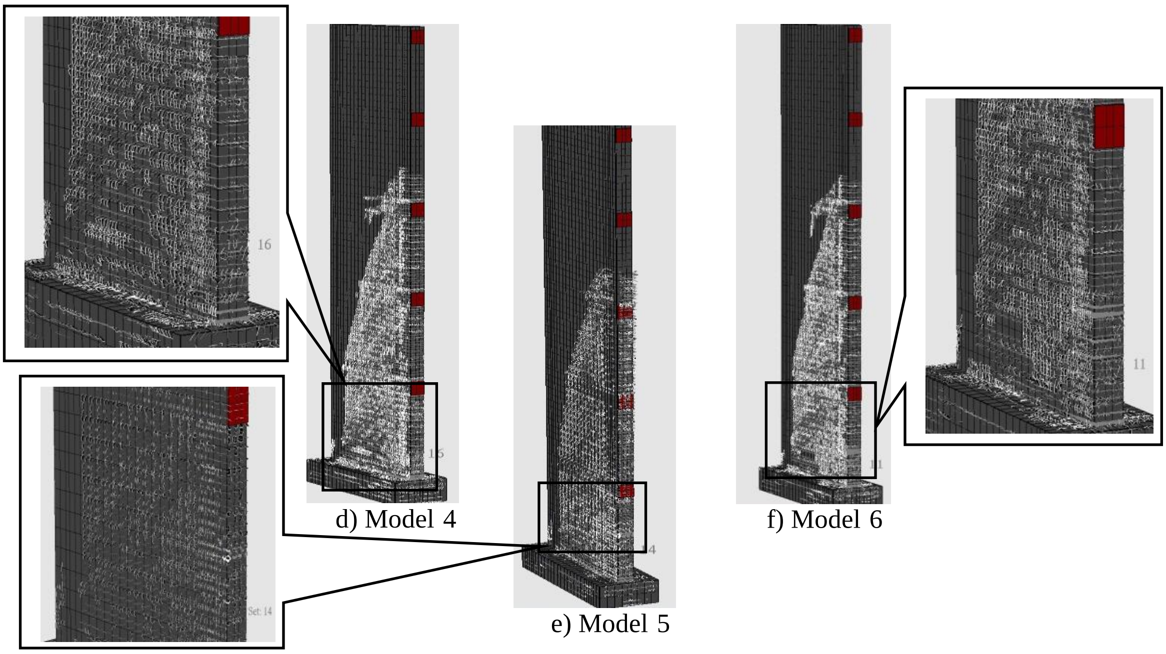
d) Model 4
e) Model 5
f) Model 6

Figure 13: Crack patterns of shear wall models prior to failure (Models 4, 5 &6)

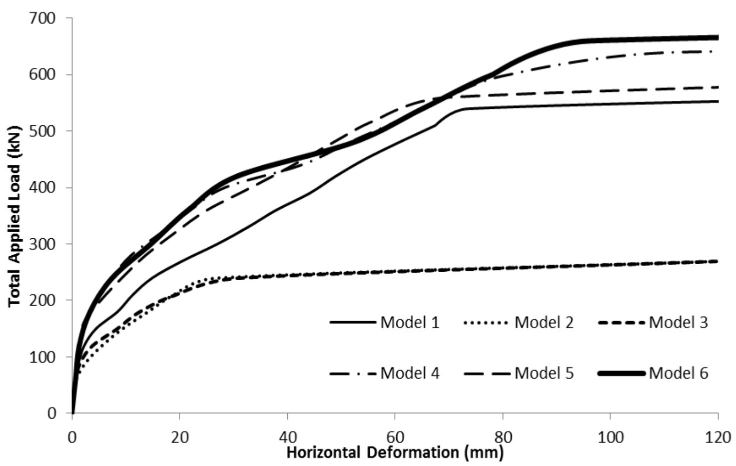

Figure 14: Comparison of shear wall models P-δ curves

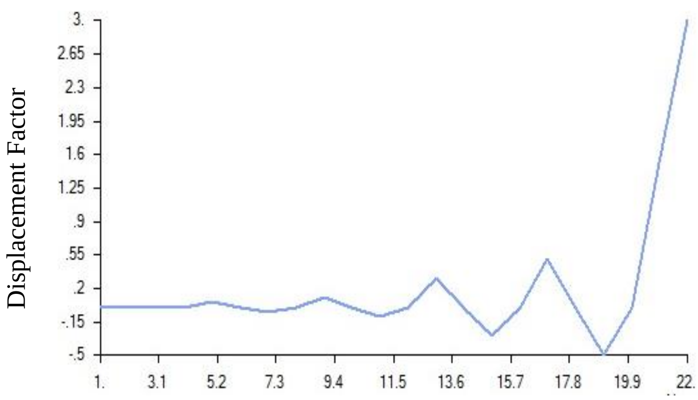

Figure 15: Displacement history curve

Figure 16 illustrates the crack patterns as they resulted from the numerical analysis. As it can be seen, opening (Figure 16a) and closing (Figure 16b) of cracks occurs according to the imposed displacements along the positive and negative x-axis. The overall hysteretic behavior is shown in Figure 17 where it is compared with the pushover analysis curve. As it derives the cyclic material model used to simulate concrete behaves in a softer manner compared to the monotonic, while managed to predict the same failure load (540kN). The opening and closing of cracks [11] cause the material to develop further deterioration thus derive a softer behavior. The full-scale 5-storey RC shear wall model required 24 hours to be analyzed for 216 load increments with an average of 10 internal iterations per load increment. This underlines the robustness of the developed algorithm [11] while the solution procedure managed to successfully converge for all load increments (the convergence criterion was set to 10^{-4}).

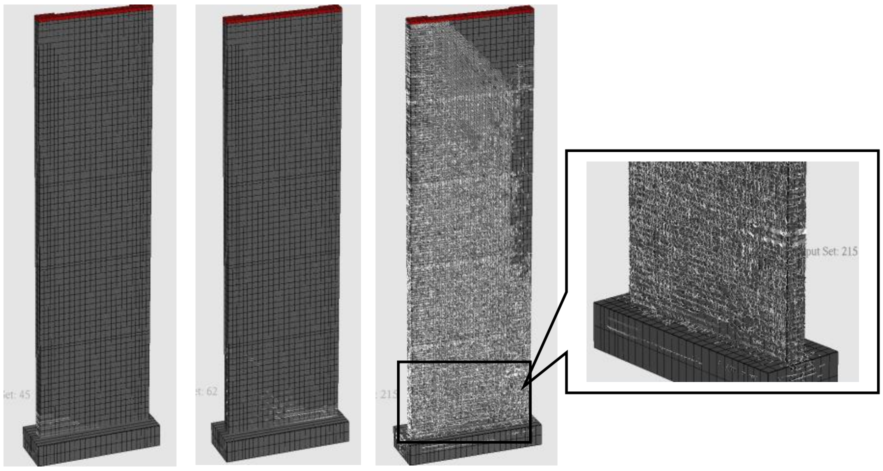

a) Cracks opening   b) Cracks closure   c) Failure

Figure 16: Crack patterns at different load step as they resulted from the cyclic analysis

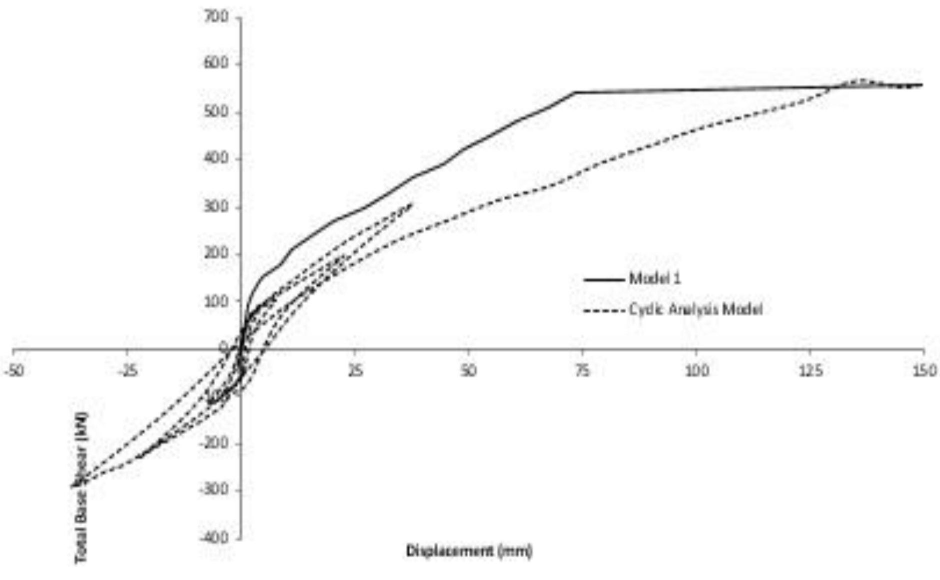

Figure 17: P-δ curves. Cyclic and monotonic analyses

6 CONCLUSIONS

The research work presented in this paper foresaw the numerical investigation of the mechanical behavior of retrofitted RC structures through the use of 3D detailed analyses. The full-scale model of a 5-storey RC building was developed prior and after retrofitting, while individual shear wall elements that were constructed to strengthen the structure (infill RC walls), were numerically investigated in an attempt to study the mechanical behavior and their overall effect on the retrofitted structure's response under seismic loads.

According to the numerical findings, the proposed strengthening design (addition of shear walls) significantly increases the seismic capacity of the structure. A single shear wall is capable in carrying the entire demand for seismic loads, while the overall increase of the seismic resistance of the structure due to retrofitting was found to be equal to 333%. The parametric investigation of the shear wall that derived after retrofitting the existing framing system, revealed the importance of proper implementation of the strengthening elements and connecting them rigidly to the existing frame. It was found that when the longitudinal rebars are not anchored properly within the existing framing system, the shear wall's overall capacity can be decreased more than 50%, leading to non-cost effective implementation.

An additional finding that derived from this research work was the overestimation of the carrying capacity of the shear wall (20%) that was computed when using the Eurocode formulae. The complexity of the derived strengthened shear wall's section that combines different types of materials and the irregular shape of the section itself, causes the development of a complicated deformation shape (bending and torsion in 3D) even for the case of symmetric horizontal loading. Evidently the proposed modeling approach will pave the way towards the development of improved guidelines and cost effective design.

From the analysis of the complete model with the initial framing geometry, it was found that it was not capable in carrying the seismic load demand while the computational robustness of the developed algorithm in handling an approximately half a million degrees of freedom numerical problem was illustrated. The computationally efficiency was found to require the implementation of a parallel solver which is a research work under process, while the effect of the interface between the existing and new concrete materials will be investigated in future projects (the detachment of the retrofitting concrete will decrease the overall strength of the structural members especially when excessive cracking will initiate). Finally, a future objective will be to perform a full-scale 5-storey RC building cyclic analysis.

REFERENCES

[1] N. Gupta, P. Dhiman and A. Dhiman, "Design and Detailing of RC Jacketing for Concrete Columns," *IOSR Journal of Mechanical and Civil Engineering,* pp. 54-58.

[2] Handbook On Sesimic Retrofit of Buildings, Central Power Works Department and Indian Building Congress in association with IIT Madras, April, 2007.

[3] H. Kaplan and S. Yılmaz, Earthquake-Resistant Structures – Design, Assessment and Rehabilitation, A. Moustafa, Ed., Rijeka: InTech, 2012.

[4] R. Zienkiewicz, "The Finite Element Method: Its Basis and Fundamentals", 6th ed., Amsterdam: Elsevier Inc, 2005.

[5] G. Markou, "ReConAn v1.00 Finite Element Analysis Software User's Manual", Athens: ISAAR, 2011.

[6] E. Orakdogen, K. Girgin, M. Baguroglu, B. Buyksisli and T. Gokce, "Performance Evaluation of a Strengthened Building Considering the Soil-Structure Interaction," *Journal of Earthquake Engineering,* 12(S2), pp. 222-233, 2008.

[7] G. Markou, R. Sabouni, F. Suleiman and R. El-Chouli, "Full-Scale Modeling of the Soil-Structure Interaction Problem Through the use of Hybrid Models," *International Journal of Current Engineering and Technology,* 5, pp. 2277-4106, 2015.

[8] M. Kotsovos. and M. Pavlovic, Structural Concrete: Finite-element analysis for limit-state design, London: Thomas Telford, 1995.

[9] G. Markou, M. Papadrakakis, "Accurate and computationally efficient 3D finite element modeling of RC structures", *Computers as Concrete,* 12(4), pp. 443-498, 2013.

[10] EN1992. Eurocode 2: Design of concrete structures, 2004.

[11] Ch. Mourlas, M. Papadrakakis and G. Markou, “Accurate and Efficient Modeling for the Cyclic Behavior of RC Structural Members”, ECCOMAS Congress, Crete Island, Greece, 5–10 June, 2016.